COMPUTATIONAL MODELING-GUIDED PRINTING OF PROANGIOGENIC HYDROGEL FOR VASCULAR PATTERNING

BY

MAX HARRISON RICH

THESIS

Submitted in partial fulfillment of the requirements
for the degree of Master of Science in Chemical Engineering
in the Graduate College of the
University of Illinois at Urbana-Champaign, 2013

Urbana, Illinois

Adviser:

Assistant Professor Hyunjoon Kong

ABSTRACT

Our living tissue is highly vascularized to facilitate transports of gaseous and bioactive molecules and subsequently ensure development, homeostasis, and remodeling processes. Cardiovascular diseases diminish the ability of vasculature to carry out these tasks and, in severe cases, cause ischemia. Cardiovascular diseases are the leading cause of human deaths worldwide, making a real need to find a way to restore the vascular blood supply where it is damaged.

Therefore, revascularization therapy has emerged to enhance treatments of a plethora of tissue defects, ischemic tissue, and acute and chronic wounds. It is common to administer various growth factors known to promote angiogenesis to target sites, often combined with biomaterials processed in the form of microporous constructs, hydrogels, or nano/micro-sized particles. These previous studies reported some impressive results to increase the number of newly formed mature blood vessels. However, revascularization therapies conducted by repeated administration of proangiogenic factors at high dosage often resulted in inadvertent formations of leaky, immature vasculature and aggregated blood vessels, termed hemangioma. It is suggested that these inadvertent results are related to physical deformation of pre-existing blood vessels where sprouting initiates and further damages on vascular wall. However, there is a lack of tools that allows us to control growth direction and spacing of vasculature and address such complications resulting from revascularization.

In this study, I hypothesized that an implantable device that can create local increase of proangiogenic growth factors in a pre-defined micropattern would allow us to control growth direction of new blood vessels and further examine their impacts on pre-

existing blood vessels. To examine this hypothesis, I printed multiple poly(ethylene glycol) diacrylate (PEGDA) hydrogel strips loaded with vascular endothelial growth factor (VEGF) using an ink-jet printer. The viscosity and surface tension of the pre-gel PEGDA solution were optimized to fabricate the gel with desired pattern. The spacing of PEGDA gel strips computationally optimized to ensure local increase of VEGF concentration in tissue which is in contact with the hydrogel strips. Finally, the printed hydrogel was implanted on a chicken chorioallantoic membrane to examine vascularization *in vivo*. Specifically, the hydrogel implant was placed between two large pre-existing blood vessels, while making the direction of hydrogel strips in parallel with or perpendicular to the pre-existing blood vessels.

I found that the orientation of the implant as well as the spacing between the printed hydrogel bars is critical in promoting the development of healthy vasculature. If the implant is designed with appropriate spacing and implanted parallel to existing vasculature, then nice healthy patterned vasculature develops. However, if the implant is placed perpendicular to existing vasculature, then pathological vasculature develops. This research goes a long way towards developing a high-throughput method to create patterned vasculature at a physiologically relevant length scale which has previously been difficult to impossible to accomplish.

TABLE OF CONTENTS

CHAPTER 1: INTRODUCTION 1
CHAPTER 2: MATERIALS AND METHODS 5
CHAPTER 3: RESULTS 10
CHAPTER 4: DISCUSSION 21
CHAPTER 5: CONCLUSION 23
REFERENCES 24

CHAPTER 1

INTRODUCTION

1.1 CARDIOVASCULAR AND ISCHEMIC DISEASES

The circulatory system is vital for nutrient supply to maintain homeostasis and organ function. Cardiovascular diseases, and the ischemic conditions associated with them (i.e. critical limb ischemia and myocardial ischemia), restrict the vascular supply of oxygen and glucose to tissues. Ischemia is characterized by insufficient nutrient supply to tissue can result in decreased organ functionality, diminished wound healing, impaired tissue regeneration, and, ultimately, necrosis, if left untreated[1]. According to the World Health Organization, cardiovascular and ischemic diseases are the leading causes of deaths world wide, contributing to approximately one-third of human deaths[2]. Thus, there is a real need to find a way to restore the supply of nutrients to ischemic tissue and prevent the damage that can come from prolonged ischemia.

1.2 THERAPEUTIC ANGIOGENESIS

Angiogenesis is the process from which new capillaries sprout from existing blood vessels. Therapeutic angiogenesis is an approach that has the potential to treat ischemic insults[3]. Angiogenesis is regulated by cytokines, including vascular endothelial growth factor (VEGF) and fibroblast growth factor (FGF)[4]. For the induction of therapeutic angiogenesis, the body's natural response is supplemented with the delivery of growth factors in order to promote tissue regeneration[3]. VEGF has been shown to have profound effects on promoting growth and expansion of vascular networks[5].

The delivery of angiogenic agents into tissues can be achieved through methods ranging from biochemical to mechanical injection. For example, VEGF can be introduced into tissues through plasmid adenoviral vectors or through direct injection[3]. While injections are feasible, a single injection requires a high dose due to the short half-life of VEGF *in vivo*. As a result, therapeutic targets can exhibit hypermermeable vessels, hypotension, and tumor growth potential[6]. Methods to provide sustained local release such as the implantation of transfected (viral or non-viral) cells can mitigate these negative side effects; however, plasmids deliver inefficient transfection and, therefore, low levels of growth factor. Adenoviral transfection is much more efficient but can elicit a host immune response, which diminishes the effectiveness of the therapy over time[3]. VEGF is known to have a dose-dependent effect. Low doses have the potential to cause leaky blood vessels, whereas, high doses can lead to hemanogioma and/or tumor formation[7].

1.3 METHODS OF DRUG DELIVERY

Drug delivery materials can be used to provide sustained and local release of VEGF. One approach is to incorporate VEGF into implantable hydrogel scaffolds at the ischemic site. Using hydrogels, the material size and chemical concentrations can be controlled to promote vessel formation on the scale of natural vessels. Within the body, each cells is within 200 μm of a capillary (8-20 μm diameter), the furthest distance over which oxygen can diffuse[8]. By replicating vasculature at this scale, tumor and hemangioma formation could possibly be prevented while promoting the establishment of a natural vasculature blood supply[9].

1.4 VASCULAR PATTERNING

Recently, the Kong group has demonstrated that electrospun polymeric fiber mesh coated with microparticles encapsulating vascular endothelial growth factor (VEGF) could develop blood vessels with larger degree of anisotropic alignment, because of local increase of VEGF along fiber orientation[9]. However, it was not possible to control vascular spacing with the electrospun fiber mesh, due to a difficulty in controlling distance between fibers. Microfabrication and stereolithography permit the formation of patterned vasculature, however, these approaches are low throughput and costly[10]. In an effort to reduce cost, increase throughput, and produce high resolution drug-releasing scaffolds, inkjet printing is employed.

1.5 RESEARCH HYPOTHESIS

I hypothesized that VEGF-releasing biomaterials fabricated in a form of micro-sized bars with controlled length and spacing using an inkjet printer would allow us to modulate both direction and spacing of newly formed blood vessels at an implantation site. Additionally, the spacing of VEGF-laden microbars should be large enough to attain local increase of the VEGF concentration in tissue at which the bars are exposed.

1.6 RESEARCH PLAN

To examine this hypothesis, poly(ethylene glycol) diacrylate (PEGDA)-based hydrogel was used as a model VEGF-releasing biomaterial. To facilitate fabrication of hydrogel microbars into a desired pattern using an inkjet printer (FIGURE 1), I formulated pre-gel ink by optimizing viscosity and surface tension with PEGDA and Pluronic

concentrations respectively. In parallel, I conducted a computational simulation to estimate the critical spacing of VEGF-encapsulating hydrogel bars above which VEGF concentration in tissue is increased locally around gel bars. Finally, hydrogel bars printed on a substrate with varied spacing was implanted on a chicken chorioallantoic membrane (CAM) to validate the computational estimation. Additionally, using the resulting hydrogel, I examined whether growth direction of capillary sprouts would influence the structural integrity and orientation of pre-existing blood vessels. Overall, the resulting inkjet printed proangiogenic hydrogel bars will greatly serve to improve quality of regeneration therapies and also better understand developmental and pathological vascularization processes.

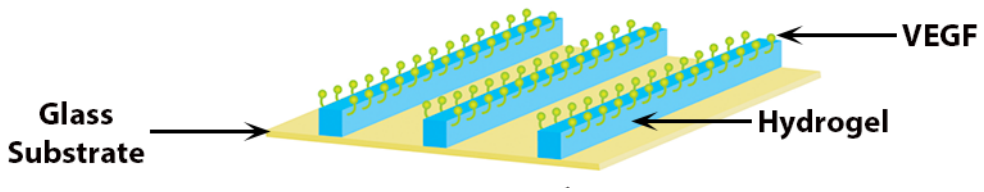

FIGURE 1: Schematic of the inkjet-printed proangiogenic hydrogel patch.

CHAPTER 2

MATERIALS AND METHODS

2.1 MATERIALS

Poly(ethylene glycol) Diacrylate (PEGDA) (M_n 700) and Pluronic® F-127 were purchased from Sigma Aldrich. Human Duo VEGF enzyme-linked immunosorbent assay (ELISA) and ELISA reagents were purchased from R&D Systems. Human recombinant VEGF 165 was purchased from R&D Systmes. Phosphate buffered saline (PBS) without magnesium and calcuium and Penicillin/Streptomycin (P/S, 10,000 U/mL/10,000 mg/mL) was purchased from Cellgro. Fertilized chicken eggs (Hy-Line W-36) were obtained from the University of Illinois Poultry Farm (Urbana, IL). Rhodamine B-Dextran (10,000 MW) was purchased from Invitrogen. Circular 18 mm cover glass no. 1 was purchased from VWR. Dimatix materials printer cartridges (DMC-11610) were purchased from Fujifilm. 3-(Trimethoxysilyl)propyl methacrylate was purchased from Sigma Aldrich. 200 proof ethyl alcohol (2701) came from Decon labs. The photoinitiator, 1-[4-(2-hydroxy-ethoxy)-phenyl]-2-hydroxy-2-methyl-1-propane-1-one (Irgacure 2959) was purchased from Ciba. Dimethyl sulfoxide (DMSO) was purchased from Fisher Scientific.

2.2 CHARACTERIZATION OF HYDROGEL PROPERTIES

Hydrogel stiffness was quantified by measuring the compressive elastic modulus (E). After incubating the gel disks in PBS for 48 hours, gel disks with a thickness of 1 mm and measuring 1 cm in diameter were compressed at a rate of 1 mm per minute using a mechanical testing system (MTS Insight). The slope of the stress versus strain curve was

used to calculate E from the first 10% of strain. The swelling ratio (Q_m) was calculated by taking the ratio of wet mass to dry mass of the gels.

2.3 Bioink Preparation

The bioink was prepared by measuring out a 4% (w/v) of PEGDA and 10% (w/v) Pluronic® solution diluted with deionized water from 100% (w/v) and 20% (w/v) solutions respectively. Additionally, 40 µL of photoinitiator at a concentration of 10 wt % in DMSO and 1 µg of VEGF were added per mL of bioink.

2.4 Bioink Characteristics

The viscosity was measured using a cone/plate viscometer (Brookfield DV II+ pro) with a low viscosity cone (spindle CPA-40Z, 20% motor power, and 23° C). A volume of 750 µL was used in order to minimize measurement error. A drop tensiometer (Attension Theta Lite) was used in order to measure the surface tension. Measurements of the surface tension were made in triplicate in order to minimize measurement error. Patterns were imaged by dissolving Rhodamine B-Dextran (10,000 MW) at a concentration of 0.5% (v/v) in the bioink and then imaged using a fluorescent microscope (Olympus BX51 Upright Fluorescence Micro).

2.5 Coverslip Preparation

Coverslips, 18 mm in diameter, were prepared for printing by first cleaning with oxygen plasma treatment. Following plasma treatment, coverslips were immersed in a 2% 3-(Trimethoxysilyl)propyl methacrylate solution diluted in 200 proof ethyl alcohol for 10

minutes to place methacrylate groups on the surface. The coverslips were next baked at 110° C on a hot plate until dry and rinsed with 200 proof ethyl alcohol. The coverslips are now ready to be chemically linked with the hydrogel ink.

2.6 Inkjet-Printing on Coverslips

Three coverslips were placed on a microscope slide, 500 μm (thick) x 75 mm (long) x 25 mm (wide), held down by 5 μL of deionized water. 1 mL of the bioink is degassed and filtered through a 0.22 μm filter before being loaded into the ink-jet cartridge (Dimatix type 11610). The best printing results were obtained by allowing the cartridge to sit overnight in a humidified chamber at 4° C prior to use.

Optimization of droplet ejection is done using the Dimatix Drop Manager software as described previously[11]. Substrate height is set to 600 μm and platen temperature control was turned off in order to print at room temperature. Patterns for printing are produced through the Drop Manager software as described previously[11]. Once printed, the slides are exposed to UV light at 254 nm for ten minutes to crosslink and then stored in PBS with 2% (v/v) P/S until use.

2.7 Drug Release

Printed hydrogel samples were prepared as above and VEGF release was compared from printed samples to bulk gels by measuring the VEGF concentration via the VEGF ELISA kit per the manufacturer's protocol. A standard curve was developed by measuring the absorbance of solutions with known VEGF concentrations and then used to determine the concentrations released at various time points from the hydrogels.

2.8 Simulation

3D finite element models for hydrogel constructs and CAM membrane were created using Comsol Multiphysics 4.1. It was assumed that the drug release kinetics of the hydrogel in the tissue membrane was governed by the Fick's first law of diffusion. Two hydrogels used in the model include (1) the arrays of 160 μm diameter half cylinders with spacing of 120 μm, (2) the arrays of 160 μm diameter half cylinders with spacing of 350 μm. The concentration of drug in the hydrogel was kept constant at $5x10^5$ mol/m^3. The CAM membrane was modeled as being 300 μm thick with a constant concentration of zero at the lower boundary of the model. This constant concentration acted as a sink, thereby consuming the VEGF once it reached the bottom surface of the model. It was assumed that hydrogel arrays were embedded in a top of the membrane. In these numerical analysis, diffusion coefficients of drug in media, tissue, and hydrogel were approximated to be 100 μm2/s, 1 μm2/s, 0.02 μm2/s, respectively. All simulations were in meters, seconds, and kilograms. Each of the samples was modeled to simulate a period of 10 days.

2.9 In Vivo Chorioallantoic Membrane (CAM) Assay for Neovascularization

Fertilized eggs were incubated horizontally at 37° C and 65% humidity for 7 days. A window was then made in the shell big enough to insert the coverslips, being careful to avoid shell fragments falling onto the membrane. Once a window was made, it was covered with scotch tape and the egg was incubated overnight at 37° C to ensure the egg's viability after making the window. The following day samples are implanted onto the CAMs of the embryos and incubated at 37° C for 7 days. Pictures of the CAM are taken after the initial

implantation and after 7 days to capture neovascularization using a Leica S6E stereomicroscope linked with a Leica D-Lux E Camera. The entire CAM assay is performed under sterile conditions.

Additionally, on the seventh day following implantation the CAM is fixed using a 4% neutral buffered formalin solution at 4° C for 2 hours. Next the CAM around the coverslip is cut out using suture scissors and imaged using the stereoscope. Finally, the fixed CAM is prepared for paraffin embedding, sectioning, and stained for α-smooth muscle actin (αSMA) using standard histological procedures. ImageJ was used to analyze images of the section and stained tissue for vessel diameter and density.

CHAPTER 3

RESULTS

3.1 INK PROPERTIES

3.1.1. Viscosity

As can be seen in Figure 2, viscosity increases as you increase the concentration of PEGDA. There is also an increase as you increase the concentration of Pluronic but the increase in viscosity as you increase the concentration of Pluronic does not have as much of a role as the increase in PEGDA concentration. Control of viscosity is important for reliable printing of patterns. When the viscosity is too low the ink jets out uncontrollably and you get patterns such as those illustrated in Figure 2B1. When the viscosity is too high the ink jets in the cartridge get clogged and you get spotty printing, as in Figure 2B3, or no printing at all. Figure 2B2 illustrates a good pattern printed with a viscosity of 12 cP.

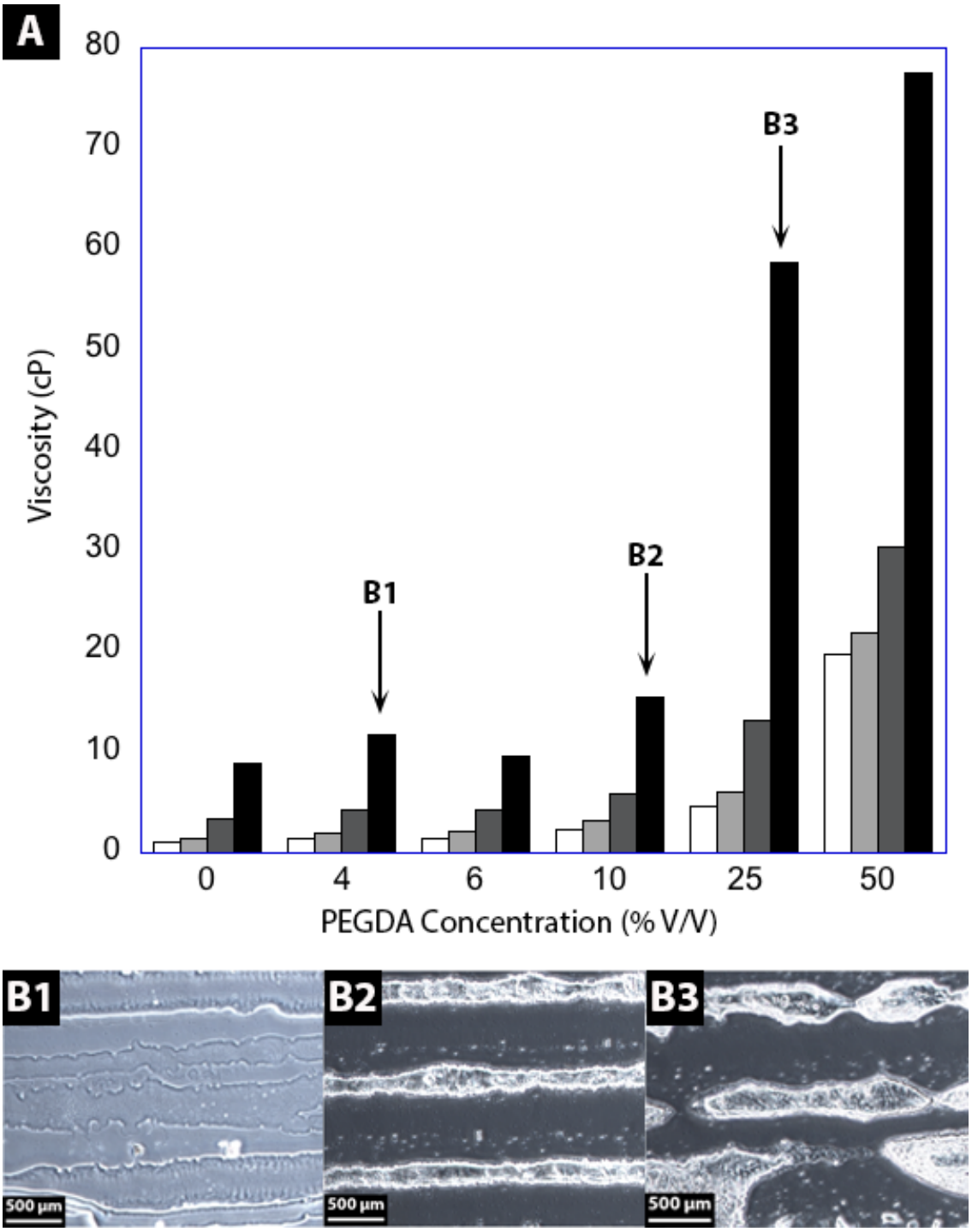

FIGURE 2: Analysis of the role of viscosity of the pre-gel solution on the quality of ink-jet printed hydrogel. (A) Effects of PEGDA concentration (V/V) on solution viscosity at a given Pluronic concentration (white = 0% Pluronic, light gray = 2% Pluronic, dark gray = 6% Pluronic, and black = 10% Pluronic). (B) Images of inket-printed hydrogels prepared wiht pre-gel solutions with viscosity of 10 cP (B1), 12 cP (B2), and 58 cP (B3). Scale bars represent 500 µm.

3.1.2 Surface Tension

As can be seen in Figure 3, with an increase in Pluronic concentration from 2% (w/v) to 10% (w/v) there is a decrease in the surface tension of the ink. As you increase the PEGDA concentration this effect of increasing the concentration of Pluronic is diminished, and appears to have no effect by time the PEGDA concentration is increased to 50% (v/v) PEGDA. A proper surface tension is also important for the printing of reliable patterns. If the surface tension is too high then droplets are not jetted in a controlled manner and you get the type of mess illustrated in Figure 3B1. When the surface tension is tuned properly, approximately 40 mN/m, then nice patterns are achievable as those in Figure 3B2.

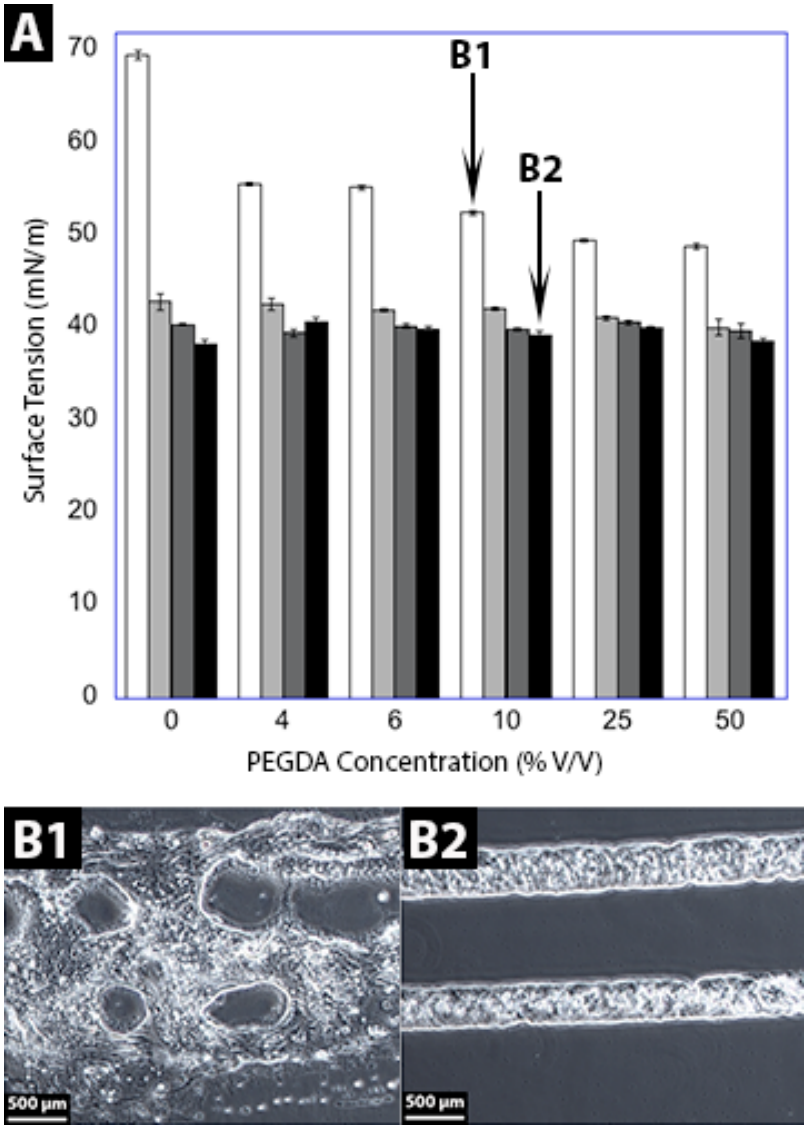

FIGURE 3: Analysis of the role of surface tension of the pre-gel solution on quality of inkjet-printed hydrogel. (A) Effects of PEGDA concentration (V/V) on surface tension at a given Pluronic concentration (white = 0% Pluronic, light gray = 2% Pluronic, dark gray = 6% Pluronic, and black = 10% Pluronic). Images of inkjet-printed hydrogels prepared with pre-gel solutions with surface tension of 55 mN/m (B1) and 40 mN/m (B2). Scale bars represent 500 µm.

3.1.3 Critical Micellization Concentration

The critical micellization concentration (CMC) of Pluronic® F127 corresponds to a solution of 0.0036 wt% in water[12]. From Figure 4B it can be seen that with the incorporation of PEGDA 700 into Pluronic solutions, I_3/I_1 begins to increase at a lower Pluronic concentration. This suggests that the presence of PEGDA alters the type of hydrophobic aggregation forming in

solution from the micelle structures formed with pure Pluronic. This is further reinforced by the shape of the Fluorescence emission spectra shown in Figures 4A1-4A3 with the broader peaks as PEGDA is incorporated into solution.

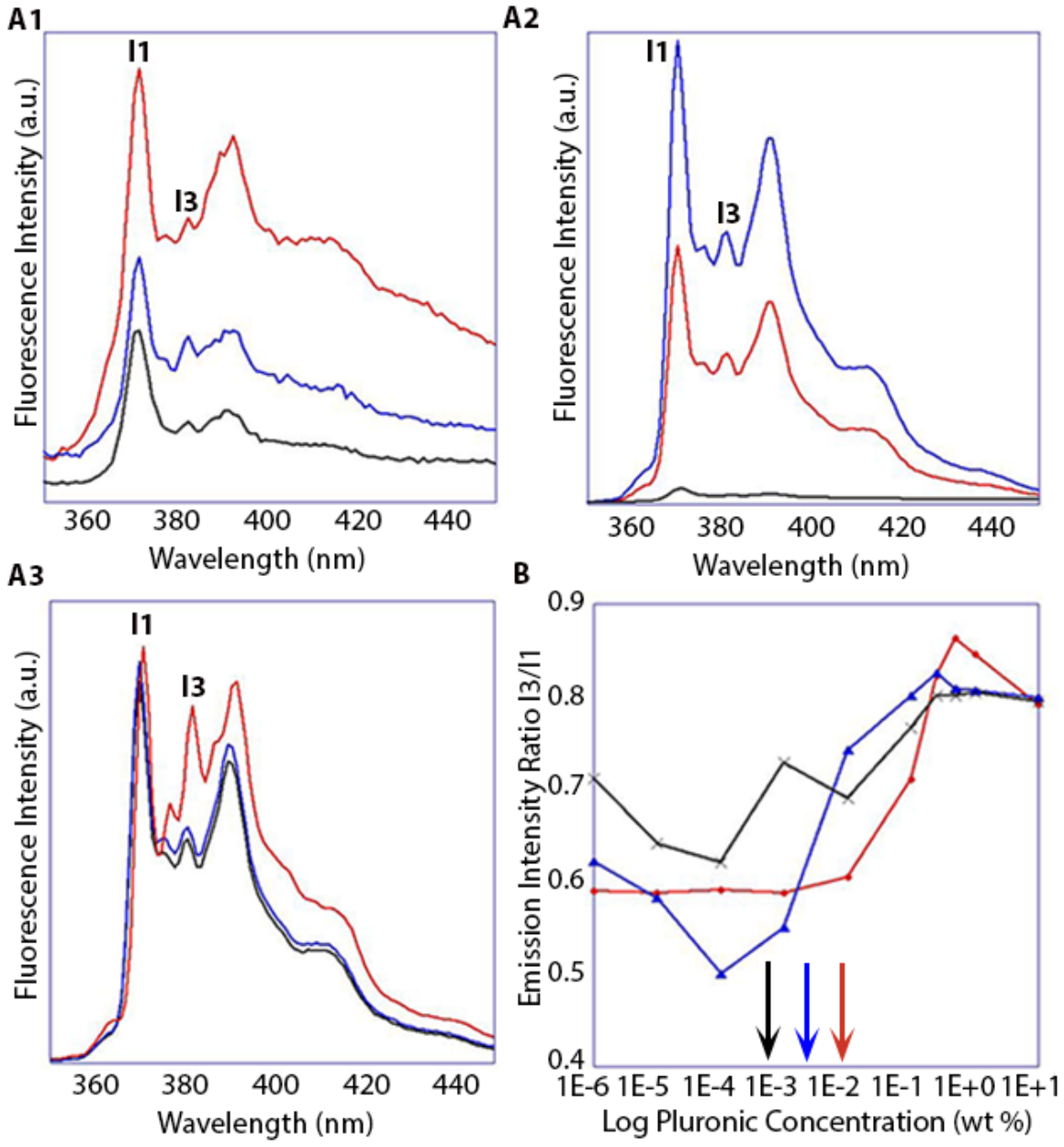

FIGURE 4: Analysis of self-association between polymers in pre-gel solutions. Fluoresence emission spectra of pyrene loaded in pre-gel solutions with a PEGDA of 25% (A1), PEGDA 4% (A2), and PEGDA 0% (A3). At a given PEGDA concentration, Pluronic concentratiosn ranged from 0.5% (red) to 0.001% (blue) to 0.000001% (black). (B) Dependency of I_3/I_1 on Pluronic concentration at a given PEGDA concentraions of 0% (red), 4% (blue), and 25% (black). The arrows correspond tot he CMC for each solution.

3.1.4 Patterns

Figure 5 represents the different types of patterns that are possible to print. The line spacing on top are 942±12 µm, 351±15 µm, and 127±13 µm respectively. The line widths are 131±8 µm, 165±9 µm, and 168±12 µm. The crossing pattern has a spacing also of 942±12 µm and line width of 131±8 µm.

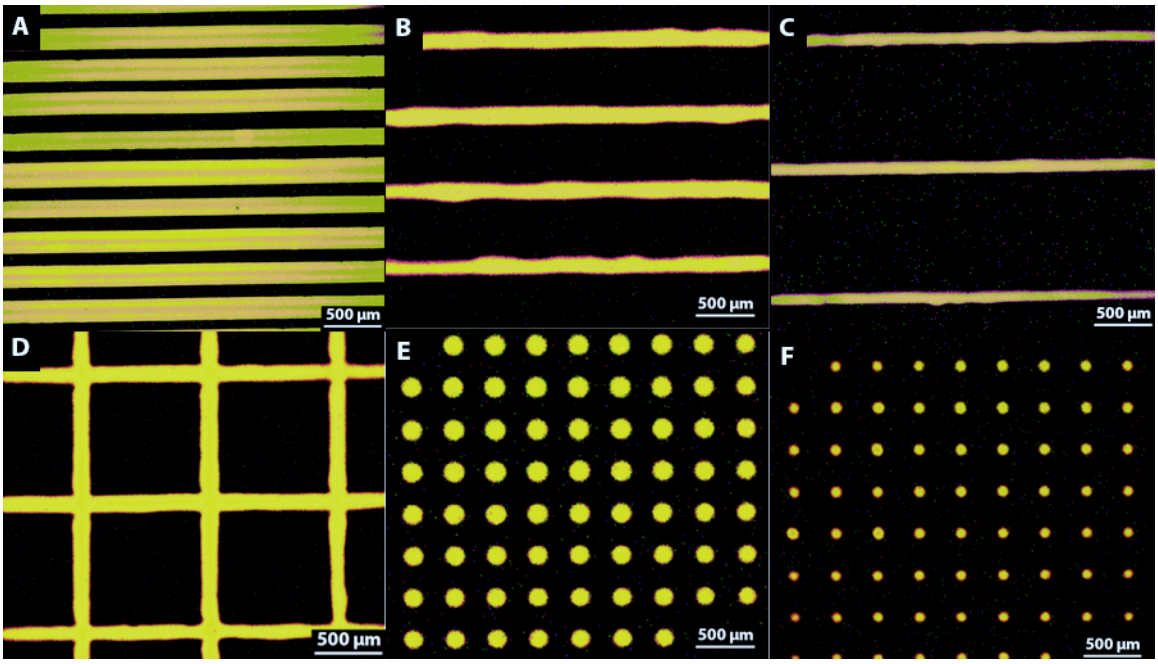

FIGURE 5: Inkjet-printed patterns. Fluorescence images of hydrogels printed into various patte4rns using a pre-gel PEGDA solution wiht a viscosity of 12 cP and surface tension of 40 mN/m. Hydrogels were labeled with rhodamine.

3.2 DRUG RELEASE

3.2.1 Simulation

Figure 6 demonstrates the simulated concentration spatial dependence on the spacing between the inkjet printed hydrogel bars. At a spacing of 120 µm, there is a constant spatial concentration distribution that is indistinguishable from a bulk gel. As the spacing is increased to 350 µm, the spatial contribution distribution mimics that of the printed pattern.

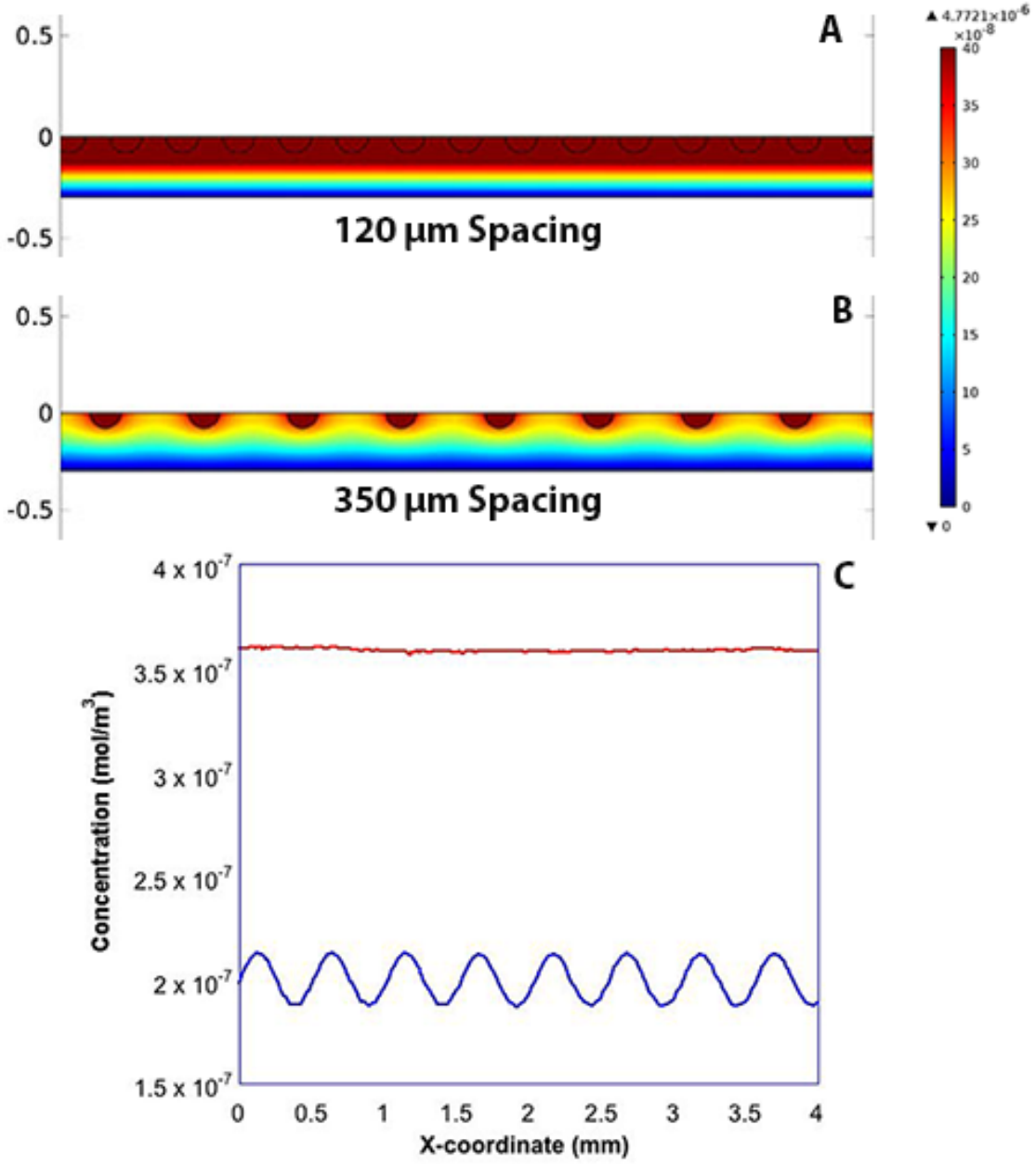

FIGURE 6: Computational simulation of VEGF release from printed hydrogel bars for optimization of spacing between bars. (A) and (B) represent the two dimension distribution of VEGF within tissues implanted with inkjet printed gel bars with spacing of 120 (A) and 350 µm (B). The tissue implanted with hydrogel bars over three days was simulated. The scale bars on the right side represent the VEGF concentration (moles/L) in tissue. (C) Analysis of one dimensional concentration of VEGF for tissue implanted with hydrogel bars with spacing of 120 (I) and 350 µm (II) following three days of implantation.

3.2.2 ELISA

Figure 7 demonstrates the profile of the VEGF release from gels. As you can see, over 7 days the 120 µm spacing printed gel and the 350 µm spacing printed gel have nearly identical release profiles whereas the bulk gel maintains a distinct release profile that releases significantly more VEGF than the printed gel patterns.

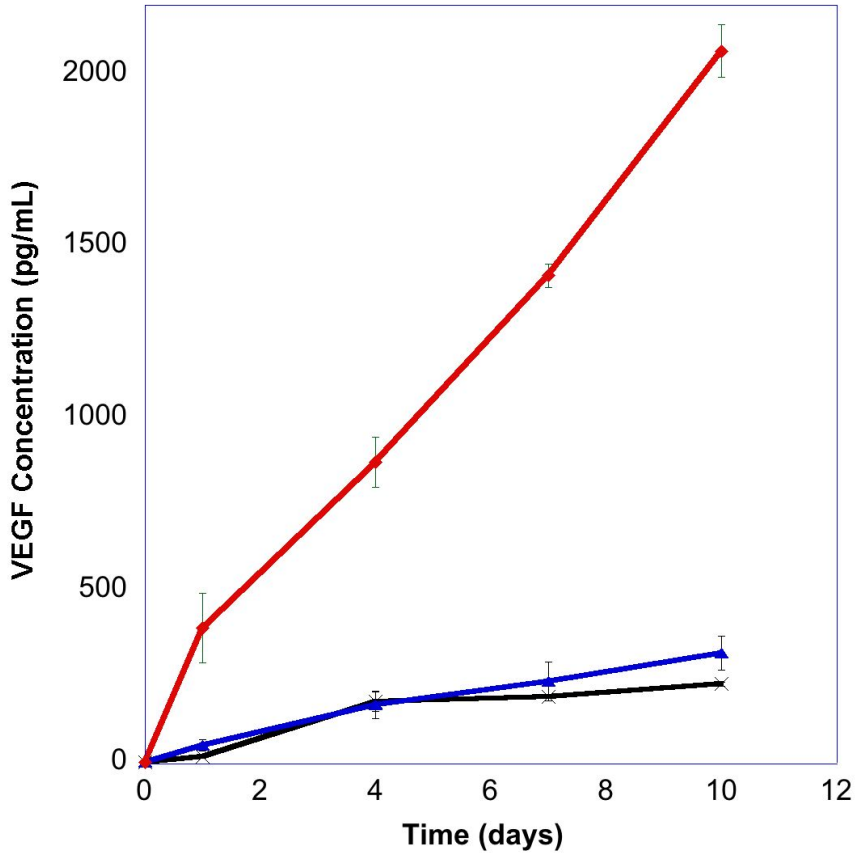

FIGURE 7: Quantification of VEGF released from bulk gel and inkjet-printed patterns. Plot of VEGF concentration versus time in days released from a linear inkjet-printed pattern with 120 µm spacing (black), a linear inkjet-printed pattern with 350 µm (blue), and a bulk gel with 10 mm diameter (red).

3.3 CAM

The orientation of how the implant is placed is also of critical importance. If the implant is placed parallel to exiting vasculature, then nice blood vessels develop, as seen in Figure 8. At the proper spacing, as demonstrated by the simulation data in Figure 6, many new blood vessels form that mimic the pattern of the printed gel (Figure 8B3). At the lower spacing of 120 μm, fewer blood vessels form and no pattern is observed (Figure 8B2). In the case of a bulk gel, even fewer blood vessel from and no patterns are observed.

Interestingly, if the implant is placed perpendicular to exiting vasculature (Figure 9A), then pathological blood vessels emerge. When the implant is first implanted the vasculature looks healthy. Following 7 days of implantation, a tortuous pattern is observed (Figure 9B) and an existing artery is ruptured (Figure 9C).

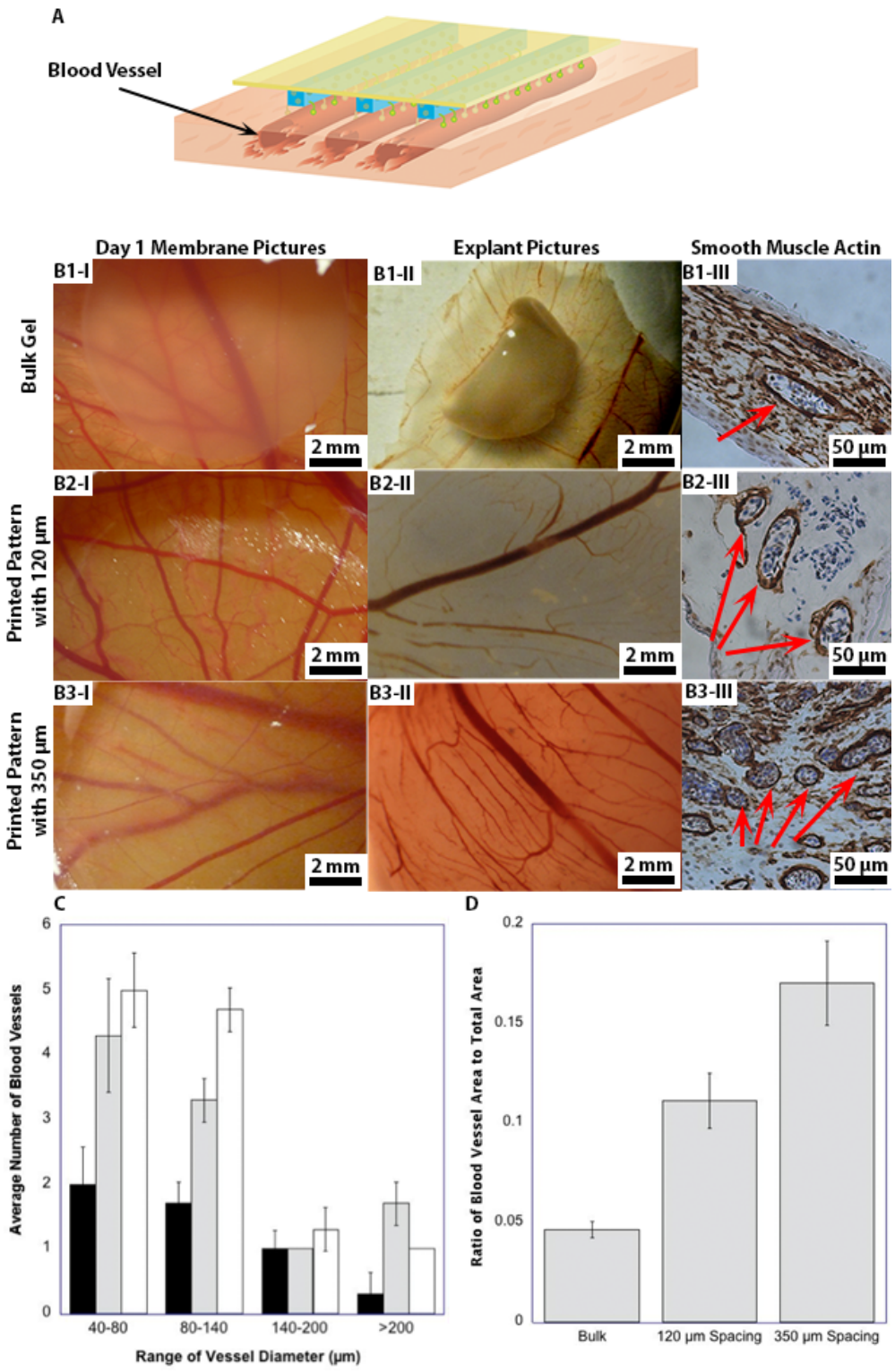

FIGURE 8: In vivo CAM analysis of effects of hydrogel bar spacing on vascularization. (A) Schematic describing hydrogel bars implanted in parallel with original arteries. (B) CAM implanted with a hydrogel disk (B-1), CAM implanted with inkjet printed hydrogel with a bar spacing of 120 µm (B-2), and CAM implanted with inkjet printed hydrogel with a bar spacing of 350 µm (B-3). Images on the first column were captured on the first day of implantation. Those on the 2nd column were captured seven days after implantation. Images on the 3rd column are cross-sectional images of CAM stained for α-smooth muscle actin. The red arrows in the 3rd column point to mature blood vessels surrounded by smooth muscle actin layer. (C) Quantitative analysis of the number of blood vessels at given diameter ranges in CAM implanted with a bulk hydrogel disk (black), inkjet-printed hydrogel with a bar spacing of120 (grey), and 350 µm (white). (D) Quantitative analysis of areal fraction of total blood vessels in CAM.

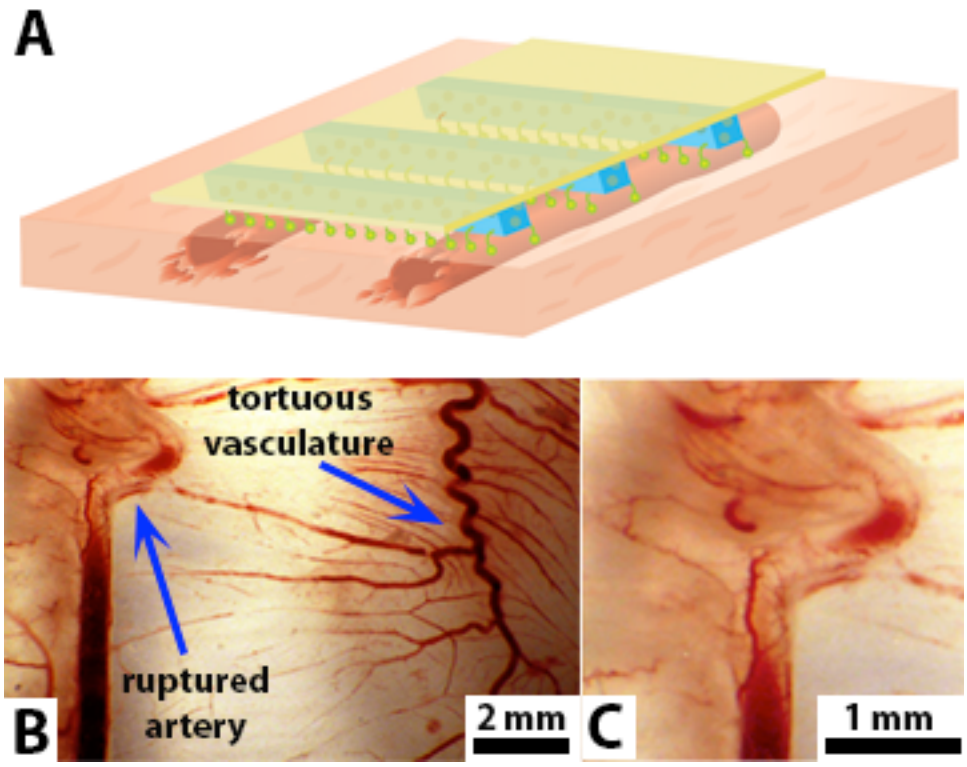

FIGURE 9:Deformation of original vasculature due to placement of hydrogel bars perpendicular to the pre-exisitng arteries. (A) Schematic describing hydrogel bars implanted perpendicular to original arteries. (B) Images of vasculature in CAM implanted with the inkjet-printed gel with a bar spacing of 350 µm. (C) is the magnified view of the ruptured artery shown in (B).

CHAPTER 4

DISCUSSION

Overall, this study demonstrates a new method to promote angiogenesis with a specific geometry and spacing at a physiologically relevant length scale. Inkjet printing requires the tight control of surface tension and viscosity in order to make large-scale reproducible patterns[11]. The viscosity needs to be low enough that it can be ejected from the nozzle, yet high enough to allow single droplets to be ejected. Surface tension must be sufficient for droplets to stay in the nozzle until ejection is desired but not too high that it prevents reliable ejection[13].

Once the optimal properties were found by tuning the concentrations of PEGDA and Pluronic in order to control viscosity and surface tension respectively, VEGF was incorporated into the ink and printed on glass substrates at length scales relevant to promote new blood vessel growth along a linear pattern. Linear patterns at such length scales have previously been very challenging to generate and have involved complicated microfabrication techniques.

The impact of the VEGF released from these patterns is dependent on both the distance between the printed hydrogel bars and the orientation of the bars compared to the orientation of the existing vasculature at the time of implanation. At shorter distances, such as the 120 µm distance, the spatial distribution of VEGF looks similar to that of a bulk gel and relatively few new blood vessels form. At a distance sufficient to create a spatial distribution of VEGF similar to the printed pattern, such as 350 µm, patterned vasculature was observed. However, if the hydrogel bars are implanted perpendicular to pre-existing vasculature, then pathogenic blood vessels develop and even disrupt the pre-existing vasculature.

This work demonstrates a novel way to recreate vasculature in a pattern with regular spacing at a physiologically relevant length scale that has not been possible before. Such work may make it possible to treat a wide variety of cardiovascular diseases without the negative side effects of current therapies.

CHAPTER 5

CONCLUSION

This study demonstrates that by carefully controlling the material properties of a pre-gel solution, namely viscosity and surface tension, it is possible to create a printable hydrogel solution that can be polymerized post printing. This hydrogel ink is capable of printing a versatile set of patterns and a variety of dimensions. The study further demonstrates that the surface area of interaction with the CAM, spacing between the patterned lines, and the orientation of the pattern all play an important role in tuning the drug delivery. Furthermore, a combination of finite element modeling and tuning the spacing between the lines to produce a pattern of drug delivery at a physiologically relevant length scale produces healthy patterned vasculature. Therefore, the study confirmed the hypothesis that VEGF-releasing inkjet printed biomaterials in the form of micro-sized bars with controlled length would allow me to modulate both direction and spacing of newly formed blood vessels at the implantation site.

Future studies should focus more on optimization of the spacing between hydrogel bars for specific therapies and on tailoring printed patterns to the specific ischemic defect being addressed. Inkjet printing offers the ability to easily print many different types of patterns and this study demonstrates that orientation of the patch to pre-existing blood vessels is critical to creating healthy new vessels and not disrupting existing vasculature. Additionally, the incorporation of other angiogenic growth factors involved in later stages of angiogenesis than VEGF may allow for the formation of more robust vessels.

REFERENCES

1. Roy, R.S., Roy, B. & Sengupta, S. Emerging technologies for enabling proangiogenic therapy. *Nanotechnology* **22**, 494004 (2011).
2. World Health Organization (2013, March). *Cardiovascular Diseases*. Retrieved from: http://www.who.int/mediacentre/factsheets/fs317/en/index.html.
3. Madeddu, P. Therapeutic angiogenesis and vasculogenesis for tissue regeneration. *Experimental Physiology* **90**, 315-326 (2005).
4. Laschke, M.W*., et al.* Angiogenesis in Tissue Engineering: Breathing LIfe into Constructed Tissue Substitutes *Tissue Engineering* **12**, 2093-2104 (2006).
5. Kaully, T., Kaufman-Francis, K., Lesman, A. & Levenberg, S. Vascularization-The Conduit to Viable Engineered Tissues. *Tissue Engineering: Part B* **15**, 159-169 (2009).
6. Naderi, H., Matin, M.M. & Bahrami, A.R. Review paper: Critical Issues in Tissue Engineering: Biomaterials, Cell Sources, Angiogenesis, and Drug Delivery Systems. *Journal of Biomaterials Applications* **26**, 383-417 (2011).
7. Phelps, E.A. & Garcia, A.J. Update on therapeutic vascularization strategies. *Regenerative Medicine* **4**, 65-80 (2009).
8. Polverini, P.J. Angiogenesis in Health and Disease: Insights into Basic Mechanisms and Therapeutic Opportunities *Journal of Dental Education* **66**, 962-975 (2002).
9. DeVolder, R.J., Bae, H., Lee, J. & Kong, H. Directed Blood Vessel Growth Using an Angiogenic Microfiber/Microparticle Composite Patch. *Advanced Materials* **23**, 3139-3143 (2011).
10. Billiet, T., Vandenhaute, M., Schelfhout, J., Van Vlierberghe, S. & Dubruel, P. A review of trends and limitations in hydrogel-rapid prototyping for tissue engineering. *Biomaterials* **33**, 6020-6041 (2012).
11. Millet, L.J., Collens, M.B., Perry, G.L.W. & Bashir, R. Pattern analysis and spatial distribution of neurons in culture. *Integrative Biology* **3**, 1167 (2011).
12. Kozlov, M.Y., Melik-Nubarov, N.S., Batrakova, E.V. & Kabanov, A.V. Relationship between Pluronic Block Copolymer Structure, Critical Micellization Concentraiton and Partitioning Coefficients of Low Molecular Mass Solutes. *Macromolecules* **33**, 3305-3313 (2000).
13. Calvert, P. Inkjet Printing for Materials and Devices. *Chemistry of Materials* **13**, 3299-3305 (2001).